

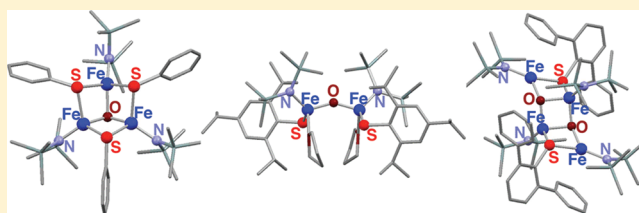
Oxido-Bridged Di-, Tri-, and Tetra-Nuclear Iron Complexes Bearing Bis(trimethylsilyl)amide and Thiolate Ligands

Shun Ohta, Saori Yokozawa, Yasuhiro Ohki, and Kazuyuki Tatsumi*

Department of Chemistry, Graduate School of Science, and Research Center for Materials Science, Nagoya University, Furo-cho, Chikusa-ku, Nagoya 464-8602, Japan

Supporting Information

ABSTRACT: A series of di-, tri-, and tetra-nuclear iron-oxido clusters with bis(trimethylsilyl)amide and thiolate ligands were synthesized from the reactions of $\text{Fe}\{\text{N}(\text{SiMe}_3)_2\}_2$ (**1**) with 1 equiv of thiol HSR ($\text{R} = \text{C}_6\text{H}_5$ (Ph), $4\text{-}^t\text{BuC}_6\text{H}_4$, $2,6\text{-Ph}_2\text{C}_6\text{H}_3$ (Dpp), $2,4,6\text{-}^i\text{Pr}_3\text{C}_6\text{H}_2$ (Tip)) and subsequent treatment with O_2 . The trinuclear clusters $[(\text{Me}_3\text{Si})_2\text{N}\{\text{Fe}\}_3(\mu_3\text{-O})\{\mu\text{-S}(4\text{-RC}_6\text{H}_4)\}_3]$ ($\text{R} = \text{H}$ (**3a**), ^tBu (**3b**)) were obtained from the reactions of **1** with HSPH or $\text{HS}(4\text{-}^t\text{BuC}_6\text{H}_4)$ and O_2 , while we isolated a tetranuclear cluster $[(\text{Me}_3\text{Si})_2\text{N}\{\text{Fe}\}_4(\mu\text{-SDpp})_2(\mu_3\text{-O})_2]$ (**4**) as crystals from an analogous reaction with HSDpp. Treatment of a tetrahydrofuran (THF) solution of **1** with HSTip and O_2 resulted in the formation of a dinuclear complex $[(\text{Me}_3\text{Si})_2\text{N}\{\text{TipS}\}(\text{THF})\{\text{Fe}\}_2(\mu\text{-O})]$ (**5**). The molecular structures of these complexes have been determined by X-ray crystallographic analysis.



INTRODUCTION

Iron-thiolate complexes have been commonly used as precursors for iron-sulfur clusters structurally analogous to those found in proteins. For example, anionic iron-thiolate complexes $[\text{Fe}(\text{SR})_4]^{2-}$ ($\text{R} = \text{alkyl or aryl group}$), which are formed from FeCl_2 and thiolate anions in polar organic solvents, react with elemental sulfur to afford various iron-sulfur clusters with $[\text{Fe}_2\text{S}_2]$, $[\text{Fe}_3\text{S}_4]$, $[\text{Fe}_4\text{S}_4]$, $[\text{Fe}_6\text{S}_6]$, and $[\text{Fe}_6\text{S}_9]$ cores.^{1,2} Non-charged iron-thiolate complexes with or without amide ligands, such as $[\text{Fe}(\text{SR})_2]$, $[\text{Fe}(\text{SR})\{\text{N}(\text{SiMe}_3)_2\}]$, and their oligomers, are available from the reactions of an iron bis-amide complex $\text{Fe}\{\text{N}(\text{SiMe}_3)_2\}_2$ (**1**) with thiols in non-polar organic solvents,^{3–8} and they also serve as good precursors for iron-sulfur clusters.^{4a,c,d,7} For example, the reaction of $\text{Fe}_3(\mu\text{-STip})_4\{\text{N}(\text{SiMe}_3)_2\}_2$ ($\text{Tip} = 2,4,6\text{-}^i\text{Pr}_3\text{C}_6\text{H}_2$) with HSTip, $\text{SC}(\text{NMe}_2)_2$, and elemental sulfur leads to the formation of an $[\text{Fe}_8\text{S}_7]$ cluster $[(\text{Me}_3\text{Si})_2\text{N}\{(\text{Me}_2\text{N})_2\text{CS}\}\text{Fe}_4\text{S}_3]_2(\mu_6\text{-S})\{\mu\text{-N}(\text{SiMe}_3)_2\}_2$ (**A**) reproducing the inorganic core of the nitrogenase P-cluster (Figure 1).^{4a,d} Another notable example is the reaction of a dinuclear iron-thiolate complex $\text{Fe}_2(\mu\text{-SDmp})_2(\text{STip})_2$ ($\text{Dmp} = 2,6\text{-}(\text{mesityl})_2\text{C}_6\text{H}_3$) with elemental sulfur to afford $[(\text{DmpS})\text{Fe}_4\text{S}_3]_2(\mu_6\text{-S})(\mu\text{-SDmp})_2(\mu\text{-STip})$ (**B**), whose framework is topologically analogous to the FeMo-cofactor of nitrogenase.^{4c} In these reactions, elemental sulfur serves not only as a sulfurization agent but also as an oxidant. The oxidation states of **A** and **B** with partial ferric character, $\text{Fe(II)}_6\text{Fe(III)}_2$ and $\text{Fe(II)}_5\text{Fe(III)}_3$, respectively, result from oxidation of the Fe(II) precursors with elemental sulfur. Similarly, one can suggest the use of O_2 instead of elemental sulfur, to synthesize iron-oxido clusters carrying thiolates.

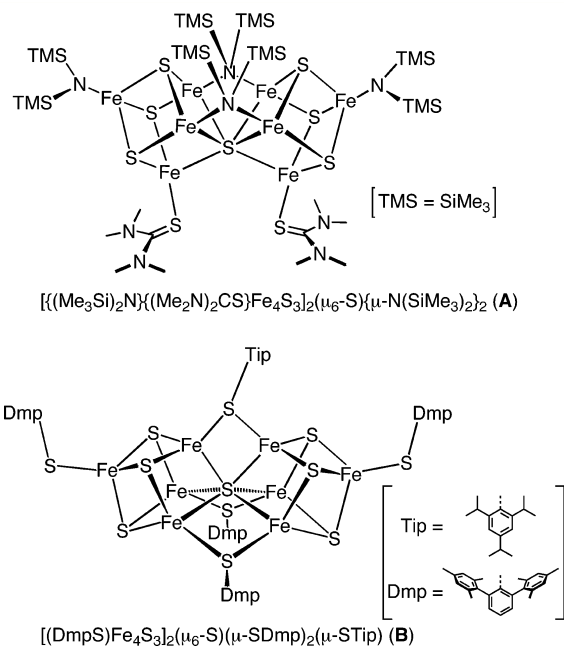


Figure 1.

Iron-oxido clusters with sulfur ligands have potential relevance to metal centers in proteins. For example, the active site of the hybrid-cluster protein (HCP) is an iron-oxido-sulfido cluster supported by cysteinyl thiolates, glutamates, and a histidyl imidazole (Figure 2).^{9,10} Iron clusters with one oxido

Received: December 1, 2011

Published: February 2, 2012



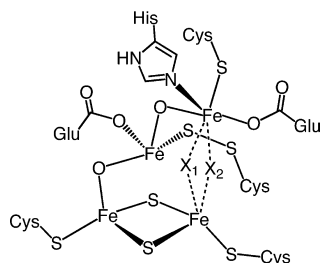


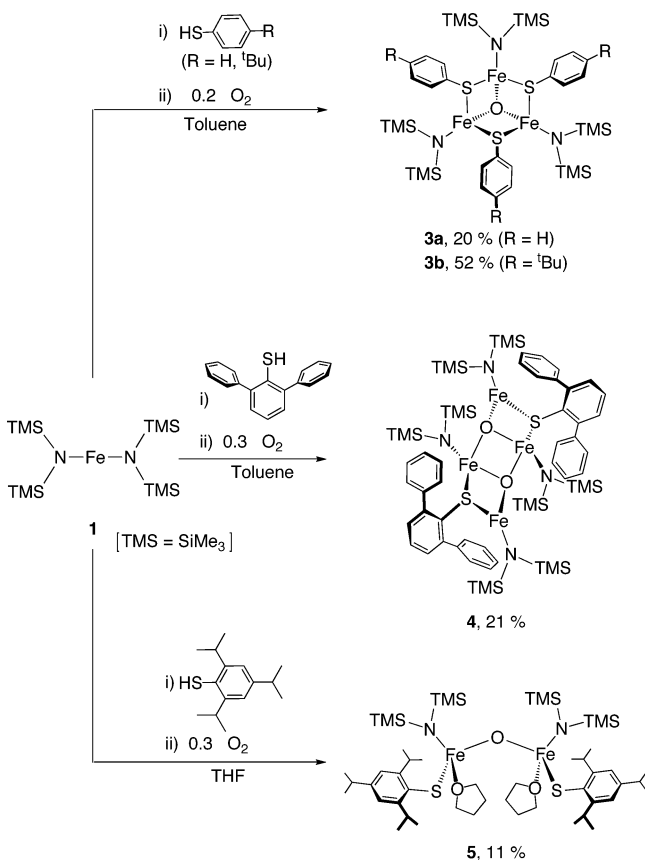
Figure 2. Active site structure of the HCP. X_1 and X_2 have been interpreted as an oxygen atom in two alternate positions.⁹

ligand may also constitute useful synthons toward synthetic analogues of the FeMo-cofactor, which consists of a $[\text{MoFe}_7\text{S}_9\text{X}]$ ($\text{X} = \text{O}, \text{N}, \text{or C}$) core featuring an iron-bound interstitial atom X .¹¹ In this study, we present a new class of iron-oxido clusters having amide and thiolate ligands, synthesized by the reactions of iron-amide-thiolate complexes with O_2 . The number of iron atoms in the products varies dependent on the thiolate ligands, and di-, tri-, and tetra-nuclear clusters were obtained.

RESULTS AND DISCUSSION

We have examined reactions of the iron bis-amide $\text{Fe}\{\text{N}(\text{SiMe}_3)_2\}_2$ (**1**) with various thiols with subsequent addition of O_2 . Scheme 1 summarizes the results.

Scheme 1



(a). Isolation of $[\{(\text{Me}_3\text{Si})_2\text{N}\}\text{Fe}_2(\mu\text{-SPh})\{\mu\text{-N}(\text{SiMe}_3)_2\}_2(\mu\text{-SPh})_2$ (2**).** The reactions of the iron bis-amide (**1**) with 1 equiv of HSAr ($\text{Ar} = \text{aryl group}$) are known to afford

the iron-amide-thiolate complexes $[\text{Fe}(\text{SAr})\{\text{N}(\text{SiMe}_3)_2\}_2]_n$. For instance, it was reported that the mono- and di-nuclear complexes $[\text{Fe}(\text{SDmp})\{\text{N}(\text{SiMe}_3)_2\}]$, $[\{(\text{Me}_3\text{Si})_2\text{N}\}\text{Fe}_2(\mu\text{-SDpp})_2]$ ($\text{Dpp} = 2,6\text{-Ph}_2\text{C}_6\text{H}_3$), and $[\{(\text{Me}_3\text{Si})_2\text{N}\}\text{Fe}_2(\mu\text{-S}\{2,6\text{-(Me}_3\text{Si)}_2\text{C}_6\text{H}_3\})_2]$ were synthesized in high yields by the 1:1 reactions of **1** and corresponding thiols.^{3b,4b,5} An iron-amide-thiolate complex with less hindered mesityl thiolates has also been isolated as a tetrahydrofuran (THF) adduct, $[\{(\text{Me}_3\text{Si})_2\text{N}\}(\text{THF})\text{Fe}_2(\mu\text{-SMes})_2]$ ($\text{Mes} = \text{mesityl}$).⁸ In an attempt to isolate an analogous iron-amide-thiolate complex for SPh or $\text{S}(4\text{-}^t\text{BuC}_6\text{H}_4)$, **1** was treated with 1 equiv of HSPH or $\text{HS}(4\text{-}^t\text{BuC}_6\text{H}_4)$ in toluene to give a dark reddish-brown suspension. From the reaction of **1** and HSPH, it was possible to obtain crystals of $[\{(\text{Me}_3\text{Si})_2\text{N}\}\text{Fe}_2(\mu\text{-SPh})\{\mu\text{-N}(\text{SiMe}_3)_2\}_2(\mu\text{-SPh})_2]$ (**2**) in 20% yield. According to the X-ray analysis, complex **2** has a linear $\text{Fe}\text{--}\text{Fe}\text{--}\text{Fe}$ array, and an inversion center resides at the midpoint of Fe2 and Fe2^* as shown in Figure 3. The inner iron atoms (Fe2 and Fe2^*) are

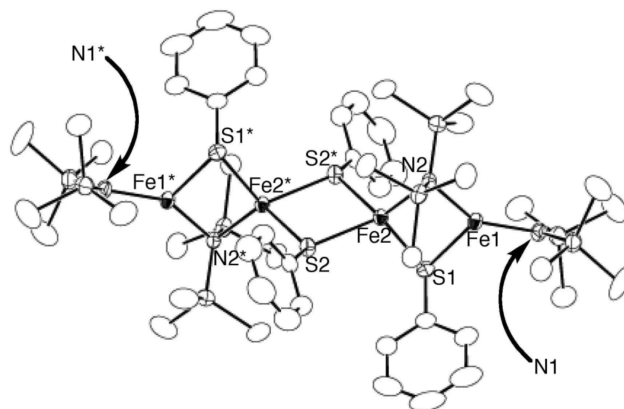


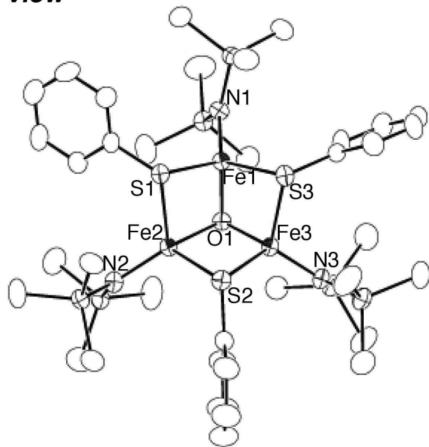
Figure 3. Molecular structure of **2** with thermal ellipsoids at the 50% probability level. Selected bond distances (Å) and angles (deg): $\text{Fe1}\text{--}\text{Fe2} = 2.7875(5)$, $\text{Fe2}\text{--}\text{Fe2}^* = 3.6352(6)$, $\text{Fe1}\text{--}\text{N1} = 1.9148(18)$, $\text{Fe1}\text{--}\text{N2} = 2.0483(15)$, $\text{Fe1}\text{--}\text{S1} = 2.3836(7)$, $\text{Fe2}\text{--}\text{N2} = 2.0544(19)$, $\text{Fe2}\text{--}\text{S1} = 2.3484(6)$, $\text{Fe2}\text{--}\text{S2} = 2.3536(7)$, $\text{Fe2}\text{--}\text{S2}^* = 2.3819(7)$, $\text{N1}\text{--}\text{Fe1}\text{--}\text{N2} = 144.11(8)$, $\text{N1}\text{--}\text{Fe1}\text{--}\text{S1} = 115.27(6)$, $\text{N2}\text{--}\text{Fe1}\text{--}\text{S1} = 100.59(6)$, $\text{N2}\text{--}\text{Fe2}\text{--}\text{S1} = 101.58(5)$, $\text{N2}\text{--}\text{Fe2}\text{--}\text{S2} = 115.80(5)$, $\text{N2}\text{--}\text{Fe2}\text{--}\text{S2}^* = 134.90(5)$, $\text{S1}\text{--}\text{Fe2}\text{--}\text{S2} = 110.54(3)$, $\text{S1}\text{--}\text{Fe2}\text{--}\text{S2}^* = 112.25(3)$, $\text{S2}\text{--}\text{Fe2}\text{--}\text{S2}^* = 79.71(2)$, $\text{Fe1}\text{--}\text{N2}\text{--}\text{Fe2} = 85.60(7)$, $\text{Fe1}\text{--}\text{S1}\text{--}\text{Fe2} = 72.18(2)$, $\text{Fe2}\text{--}\text{S2}\text{--}\text{Fe2}^* = 100.29(2)$.

four-coordinate and are bound to three bridging thiolate sulfurs and one bridging amide nitrogen, while the outer iron atoms (Fe1 and Fe1^*) are three-coordinate with one terminal amide, a bridging amide, and a bridging thiolate. The $\text{Fe1}\text{--}\text{Fe2}$ distance of $2.7875(5)$ Å is notably shorter than the $\text{Fe2}\text{--}\text{Fe2}^*$ distance of $3.6352(6)$ Å. The short $\text{Fe1}\text{--}\text{Fe2}$ distance is accompanied by the acute $\text{Fe1}\text{--}\text{S1}\text{--}\text{Fe2}$ angle of $72.18(2)^\circ$, while the $\text{Fe2}\text{--}\text{S2}\text{--}\text{Fe2}^*$ angle is large ($100.29(2)^\circ$), indicating a weak $\text{Fe1}\text{--}\text{Fe2}$ interaction. The molecule may be viewed as a dimer of the $[\{(\text{Me}_3\text{Si})_2\text{N}\}(\text{PhS})\text{Fe}_2(\mu\text{-SPh})\{\mu\text{-N}(\text{SiMe}_3)_2\}]$.

(b). Reaction of **1 with HSPH or $\text{HS}(4\text{-}^t\text{BuC}_6\text{H}_4)$ in the Presence of O_2 .** We observed that a dark reddish-brown toluene suspension, which was obtained from the reaction of **1** and 1 equiv of HSPH or $\text{HS}(4\text{-}^t\text{BuC}_6\text{H}_4)$, turned to a dark brown solution, upon treatment with 0.2 equiv of O_2 . From the resulting solution, the trinuclear oxido complexes $[\{(\text{Me}_3\text{Si})_2\text{N}\}\text{Fe}_3(\mu_3\text{-O})\{\mu\text{-S}(4\text{-RC}_6\text{H}_4)\}_3]$ were isolated in 20% (**3a**; $\text{R} = \text{H}$) and 52% (**3b**; $\text{R} = ^t\text{Bu}$) yields, respectively, as dark brown crystals (Scheme 1, top). Crystals suitable for X-

ray diffraction study were obtained from hexane for **3a** and **3b**. Both **3a** and **3b** crystallize in the space group of $P\bar{1}$ (#2) with $Z = 4$, so there are two crystallographically independent molecules in an asymmetric unit. As the molecular structures of **3a** and **3b** are very similar, top and side views of only one of the independent molecules of **3a** are shown in Figure 4.

Top view



Side view

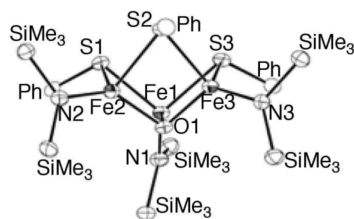


Figure 4. Molecular structure of **3a** with thermal ellipsoids at the 50% probability level. In the side view, methyl and phenyl (except ipso carbon atom) groups have been omitted for clarity. Selected bond distances (Å) and angles (deg): Fe1–Fe2 = 2.8745(8), Fe1–Fe3 = 2.9346(8), Fe2–Fe3 = 2.9325(8), Fe1–N1 = 1.872(2), Fe2–N2 = 1.872(2), Fe3–N3 = 1.911(2), Fe1–S1 = 2.3892(8), Fe1–S3 = 2.3399(10), Fe2–S1 = 2.4037(9), Fe2–S2 = 2.3493(10), Fe3–S2 = 2.4556(8), Fe3–S3 = 2.4692(7), Fe1–O1 = 1.895(2), Fe2–O1 = 1.899(2), Fe3–O1 = 1.984(2), Fe1–O1–Fe2 = 98.51(8), Fe1–O1–Fe3 = 98.32(9), Fe2–O1–Fe3 = 98.07(9).

Clusters **3a** and **3b** consist of a nearly-equilateral triangle Fe_3 frame, to which an oxygen atom caps, and three thiolate sulfur atoms bridge the iron atoms, and one amide coordinates at each iron from the lateral site. The coordination geometry of each iron is tetrahedral. The $\mu_3\text{-O}$ atom of **3a** or **3b** is displaced by 0.934(3)–0.950(2) Å from the Fe_3 plane. This is in contrast to the known $\text{Fe}_3(\mu_3\text{-O})$ clusters with octahedral Fe(II)Fe(III)_2 atoms,^{12–14} in which the $\mu_3\text{-O}$ ligand is located only ≤ 0.34 Å from the Fe_3 plane. In agreement with the structural difference between **3a–b** and the known $\text{Fe}_3(\mu_3\text{-O})$ clusters, the $\text{Fe}-(\mu_3\text{-O})\text{-Fe}$ angles of **3a–b** (97.17(13)–98.69(13)°) are smaller than those of the known $\text{Fe}_3(\mu_3\text{-O})$ clusters (109.9(2)–127.1(4)°).^{12–14} The amide nitrogens in **3a–b** are planar, and deviation of the N atom from the plane defined by the neighboring silicon and iron atoms is $\leq 0.043(3)$ Å. The Si–N–Si planes orient nearly perpendicular to the Fe_3 plane (74.3–98.7°) because of steric hindrance with $\mu\text{-SR}$ ligands. Synthesis of the sulfido analogues of **3a–b**, $[\{(\text{Me}_3\text{Si})_2\text{N}\}\text{Fe}]_3(\mu_3\text{-S})(\mu\text{-SR})_3$ ($\text{R} = 4\text{-CH}_3\text{C}_6\text{H}_4$, adamantyl), from the reactions of **1**

with the corresponding thiols and elemental sulfur has been reported.⁷

The oxidation state of **3a–b** is Fe(II)Fe(III)_2 , and their cyclic voltammograms (CVs) exhibit one quasi-reversible oxidation and one reduction events as shown in Figure 5. The half-

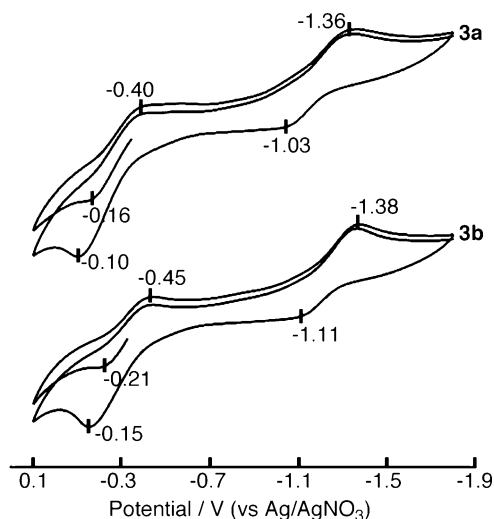


Figure 5. CVs (scan rate = 0.1 V/s) of **3a** (top) and **3b** (bottom) in THF.

potentials ($E_{1/2}$) for the $\text{Fe(III)}_3/\text{Fe(II)Fe(III)}_2$ couple are at $E_{1/2} = -0.28$ V (**3a**) and -0.33 V (**3b**), and those for the $\text{Fe(II)Fe(III)}_2/\text{Fe(II)}_2\text{Fe(III)}$ couple are at $E_{1/2} = -1.20$ V (**3a**) and -1.25 V (**3b**). The redox potentials of **3b** are slightly more negative compared with the corresponding potentials of **3a**, probably because of the electron-donating property of the thiolate $t\text{Bu}$ groups.

(c). Reaction of 1 with HSDpp (Dpp = 2,6- $\text{Ph}_2\text{C}_6\text{H}_3$) in the Presence of O_2 . A 1:1 reaction mixture of **1** and HSDpp in toluene was treated with O_2 (0.3 equiv to **1**) at room temperature resulting in a dark purple solution. The solution color gradually turned to dark reddish brown. Recrystallization of the crude product from toluene/hexane gave black block crystals of the tetranuclear oxido complex $[\{(\text{Me}_3\text{Si})_2\text{N}\}_2\text{Fe}_2(\mu\text{-SDpp})_2(\mu_3\text{-O})_2$ (**4**) in 21% yield (Scheme 1, middle), along with colorless crystals of the disulfide Dpp–SDpp which was isolated in 20% yield. The formation of DppS–SDpp accounts for the reduction of iron. Cluster **4** is formed via 4e reduction of O_2 to give two $\mu_3\text{-oxido}$ ligands. Two of the required electrons are furnished by iron oxidation from 2Fe(II)_2 to the $\text{Fe(II)}_2\text{Fe(III)}_2$ state of **4**, and the formation of DppS–SDpp supplies the other $2e^-$. This $\text{Fe(II)}_2\text{Fe(III)}_2$ state of **4** appears to be stable, according to its CV, which shows only an irreversible reduction event at -2.48 V vs Ag/AgNO_3 .

X-ray analysis of **4** reveals an $\text{Fe}_4(\mu_3\text{-O})_2$ framework, as shown in Figure 6. The atoms Fe1, O, Fe1*, and O* form a nearly perfect square face, which has an inversion center at its middle. Fe2 and Fe2* are mutually trans with respect to the $[\text{Fe}_2\text{O}_2]$ plane, with the Fe2–O distance of 1.9358(10) Å. The Fe1–Fe1* distance (2.7139(4) Å) is much shorter than the Fe1–Fe2 distance (3.0223(4) Å), which is too long to be a direct Fe–Fe interaction. The central iron atoms (Fe1 and Fe1*) are close to tetrahedral, coordinated by two oxido ligands, one SDpp, and one amide. Although the outer iron atoms (Fe2 and Fe2*) seem to be three-coordinate with oxido, SDpp, and amide ligands, an additional weak interaction

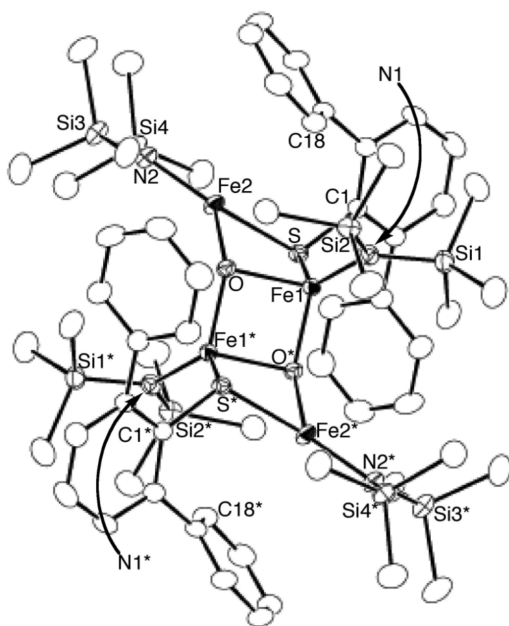


Figure 6. Molecular structure of $4\text{-C}_6\text{H}_{14}$ with thermal ellipsoids at the 50% probability level. Selected bond distances (Å) and angles (deg): Fe1–Fe1* = 2.7139(4), Fe1–Fe2 = 3.0223(4), Fe1–N1 = 1.8834(13), Fe1–S = 2.3870(5), Fe1–O = 1.9310(13), Fe1–O* = 1.8998(10), Fe2–N2 = 1.9089(15), Fe2–S = 2.4336(6), Fe2–O = 1.9358(10), Fe2–C18 = 2.9382(16), O–Fe1–O* = 89.79(5), Fe1–N1–Si1 = 115.30(10), Fe1–N1–Si2 = 122.97(9), Si1–N1–Si2 = 121.35(8), Fe2–N2–Si3 = 116.24(8), Fe2–N2–Si4 = 119.75(11), Si3–N2–Si4 = 123.83(10), Fe1–S–Fe2 = 77.644(17), Fe1–S–C1 = 117.19(6), Fe2–S–C1 = 119.74(7), Fe1–O–Fe2 = 102.81(6), Fe1–O–Fe1* = 90.21(5), Fe2–O–Fe1* = 134.86(6).

between Fe2 and one of the phenyl groups of the SDpp ligand with a shortest Fe–C distance of 2.9382 (16) Å is not negligible. This weak iron-phenyl interaction leads to a slight pyramidalization of Fe2, and Fe2 deviates by 0.2962(3) Å from the least-square plane defined by amide nitrogen (N2), thiolate sulfur (S), and oxygen (O) atoms. Similar weak Fe–C(arene) interactions have been found in iron complexes having S(2,6- $\text{Ar}_2\text{C}_6\text{H}_3$) ligands,^{3b,c,4b,c,15} but usually their closest Fe–C(arene) distances (2.272(2)–2.589(2) Å) are shorter than that of **4**. Cluster **4** contains two kinds of iron sites Fe1/Fe1* and Fe2/Fe2* with a $\text{Fe}(\text{II})_2\text{Fe}(\text{III})_2$ mixed oxidation state, and notably the Fe1–N (1.8834 (13) Å), Fe1–S (2.3870(5) Å), and Fe1–O distances (1.8998(10) and 1.9310(13) Å) are shorter than the Fe2–N (1.9089(15) Å), Fe2–S (2.4336(6) Å), and Fe2–O (1.9358(10) Å) distances. This difference may indicate that Fe1/Fe1* are ferric sites and Fe2/Fe2* are ferrous sites. Thus far, several $\text{Fe}_4(\mu_3\text{-O})_2$ clusters have been reported, and most of the precedent clusters consist of octahedral $\text{Fe}(\text{III})_4$ centers with bridging carboxylate ligands.¹⁶ Cluster **4** is a unique type of $\text{Fe}_4(\mu_3\text{-O})_2$ cluster because of its tetrahedral iron atoms in the mixed $\text{Fe}(\text{II})_2\text{Fe}(\text{III})_2$ oxidation state and the presence of thiolate ligands.

(d). Reaction of **1 with HSTip (Tip = 2,4,6- $\text{Pr}_3\text{C}_6\text{H}_2$) in the Presence of O_2 .** The reaction of **1** with 1 equiv of HSTip in THF at room temperature followed by treatment with 0.3 equiv of O_2 at -40°C resulted in the formation of an $\text{Fe}(\text{III})_2 \mu\text{-oxido}$ complex $[\{(\text{Me}_3\text{Si})_2\text{N}\}(\text{TipS})(\text{THF})\text{Fe}]_2(\mu\text{-O})$ (**5**), which crystallized as red needles in 11% yield (Scheme 1, bottom). In the CV of **5** in THF, only an irreversible reduction process was observed at -1.65 V vs Ag/AgNO_3 . The UV–vis

spectrum of **5** in hexane exhibited two broad absorptions at 429 nm ($\epsilon = 6100 \text{ M}^{-1} \text{ cm}^{-1}$) and 330 nm ($\epsilon = 6300 \text{ M}^{-1} \text{ cm}^{-1}$), in addition to a shoulder at 280 nm ($\epsilon = 9200 \text{ M}^{-1} \text{ cm}^{-1}$). The former two bands are probably ascribed to the charge-transfer bands from amide, thiolate, and/or oxido ligands to $\text{Fe}(\text{III})$.

The Fe–O–Fe structure of **5** was identified by X-ray crystallographic analysis (Figure 7). In the solid state, cluster **5**

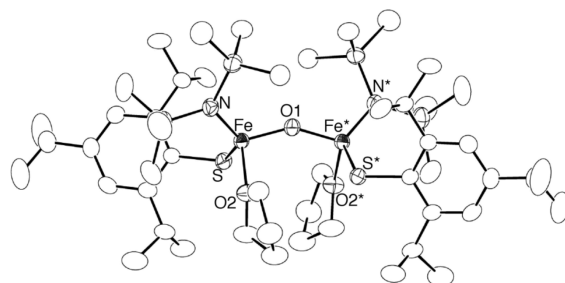


Figure 7. Molecular structure of **5** with thermal ellipsoids at the 50% probability level. Selected bond distances (Å) and angles (deg): Fe–N = 1.913(3), Fe–S = 2.2798(12), Fe–O1 = 1.7845(9), Fe–O2 = 2.067(2), N–Fe–S = 126.05(10), N–Fe–O1 = 117.34(12), N–Fe–O2 = 102.62(14), S–Fe–O1 = 100.74(4), S–Fe–O2 = 105.33(9), O1–Fe–O2 = 101.85(9), Fe–O1–Fe* = 149.3(2).

is in a C_{2v} symmetry, with a C_2 axis running through the μ -oxido ligand. A THF molecule is bound to each iron atom, and the iron atom has a slightly distorted tetrahedral $\text{Fe}(\text{N})(\text{O})_2(\text{S})$ geometry. The Fe–O–Fe* angle ($149.3(2)^\circ$) and the Fe–O distance (1.7845(9) Å) are within the ranges of those reported for $\text{Fe}^{\text{III}}\text{–O–Fe}^{\text{III}}$ complexes, $131.7\text{--}180^\circ$ for Fe–O–Fe and $1.7266(4)\text{--}1.792(1)$ Å for Fe–O.^{17–19} The Fe–S distance of **5** (2.2798(12) Å) is comparable to those of $[(\text{PhS})_3\text{Fe–O–Fe}(\text{SPh})_3]^{2-}$ (2.287(2)–2.305(2) Å).²⁰ The N–Fe–O angles ($102.62(14)\text{--}117.34(12)^\circ$) and the N–Fe–S angle ($126.05(10)^\circ$) are larger than the S–Fe–O angles ($100.74(4)\text{--}105.33(9)^\circ$) and the O–Fe–O angle ($101.85(9)^\circ$), probably because of the steric hindrance of the amide ligand.

CONCLUDING REMARKS

The reactions of complex **1** with thiols and O_2 provide a new class of iron-oxido clusters carrying amide and thiolate ligands, and the number of iron atoms in the clusters varies dependent on the thiolate ligands. This work offers a new synthetic route to iron-oxido clusters carrying sulfur ligands; however further work will be required to model some metal clusters in biology. For example, the reactions of iron-thiolate-amide complexes with a mixture of O_2 and elemental sulfur are probably important to provide synthetic analogues of the active site of the HCP. The reactions of **3a–b** with iron and molybdenum compounds together with elemental sulfur may provide Mo/Fe/S/O clusters relevant to the FeMo-cofactor. These studies are currently on going in our group.

EXPERIMENTAL SECTION

General Procedures. All reactions except for the synthesis of DppS–SDpp were carried out using standard Schlenk techniques and a glovebox under a nitrogen atmosphere. Hexane, hexamethyldisiloxane (HMDSO), toluene, and THF were purified by the method of Grubbs et al.,²¹ where the solvents were passed over columns of activated alumina and a supported copper catalyst supplied by Hansen & Co. Ltd. Dry cyclohexane was purchased from Kanto Chemical Co., Inc., and was used as received. UV–vis spectra were measured on a JASCO V560 spectrometer. Elemental analyses were recorded on a

Table 1. Crystal Data for 2, 3a–b, 4·C₆H₁₄, 5, and DppS–SDpp

	2	3a	3b	4·C ₆ H ₁₄	5	DppS–SDpp
formula	C ₄₈ H ₉₂ Fe ₄ N ₄ S ₄ Si ₈	C ₃₆ H ₆₉ Fe ₃ N ₃ OS ₃ Si ₆	C ₄₈ H ₉₃ Fe ₃ N ₃ OS ₃ Si ₆	C ₆₆ H ₁₁₂ Fe ₄ N ₄ O ₂ S ₂ Si ₈	C ₅₀ H ₉₈ Fe ₂ N ₂ O ₃ S ₂ Si ₄	C ₃₆ H ₂₆ S ₂
fw	1301.59	992.19	1160.51	1505.82	1063.49	522.72
temperature	−100	−100	−100	−100	−100	−100
crystal system	triclinic	triclinic	triclinic	triclinic	monoclinic	monoclinic
space group	$P\bar{1}$ (#2)	$P\bar{1}$ (#2)	$P\bar{1}$ (#2)	$P\bar{1}$ (#2)	C2/c (#15)	P2 ₁ /a (#14)
a (Å)	9.3519(14)	14.621(2)	15.234(3)	12.6761(12)	34.823(8)	17.587(3)
b (Å)	12.756(2)	15.555(3)	19.699(3)	13.1696(8)	10.771(2)	13.356(3)
c (Å)	14.818(2)	23.629(4)	22.889(4)	13.2939(10)	19.696(5)	23.862(5)
α (deg)	82.532(6)	82.513(5)	73.301(6)	65.161(4)		
β (deg)	78.884(5)	87.754(7)	80.481(7)	81.878(4)	122.306(3)	103.347(3)
γ (deg)	81.637(5)	77.228(5)	89.422(7)	84.077(5)		
V (Å ³)	1706.6(5)	5195.9(16)	6483.7(18)	1991.4(3)	6244(2)	5453.5(17)
Z	1	4	4	1	4	8
D _{calc} (g cm ^{−3})	1.266	1.268	1.198	1.256	1.131	1.273
μ(MoKα) (cm ^{−1})	11.273	11.133	9.019	9.269	6.437	2.191
2θ _{max} (deg)	55.0	55.0	55.0	55.0	55.0	55.0
no. of data collected	13633	41948	78261	23932	24801	42906
no. of unique rflns	7431	22741	29422	9048	7134	12251
no. of variables	307	938	1123	388	334	685
R ₁ ^a	0.0325	0.0643	0.0792	0.0289	0.0626	0.0626
wR ₂ ^b	0.0873	0.1975	0.2348	0.0860	0.1868	0.1702
GOF ^c	1.041	1.152	1.044	1.058	1.004	1.106

^a $I > 2\sigma(I)$, $R_1 = \sum |F_o| - |F_c| / \sum |F_o|$. ^bRefined with all data, $wR_2 = [\sum w(F_o^2 - F_c^2)^2] / [\sum w(F_o^2)^2]^{1/2}$. ^cGOF = $[\sum w(F_o^2 - F_c^2)^2] / (N_o - N_p)^{1/2}$, where N_o and N_p denote the numbers of reflection data and parameters.

LECO-CHNS-932 elemental analyzer where the crystalline samples were sealed in silver capsules under nitrogen. CVs were recorded in THF at room temperature using gold as the working electrode with 0.2 M [ⁿBu₄N][PF₆] as the supporting electrolyte. The potentials are referenced to Ag/AgNO₃. The ¹H NMR (600 MHz) and the ¹³C{¹H} NMR (151 MHz) were recorded on a JEOL ECA600 spectrometer. The ¹H and the ¹³C{¹H} NMR chemical shifts are given in parts per million (ppm) relative to the residual signals of the deuterated solvents. Fe[N(SiMe₃)₂]₂ (1),²² HSDpp,²³ and HSTip²⁴ were prepared according to literature procedures. HSPH and HS-(4'-BuC₆H₄) were purchased and used as received.

Synthesis of [(Me₃Si)₂N]Fe₂(μ-SPh)(μ-N(SiMe₃)₂)₂(μ-SPh)₂ (2). A toluene (5 mL) solution of HSPH (0.3 mL, 2.93 mmol) was added dropwise to a toluene (5 mL) solution of 1 (1.10 g, 2.92 mmol) at 0 °C. The reaction mixture became a dark reddish-brown suspension immediately and was allowed to warm to room temperature. After stirring at this temperature for 12 h, the mixture was centrifuged to remove insoluble material. Upon standing the solution at −40 °C, dark orange plates of 2 (0.045 g, 5%) were formed. The mother liquor was concentrated and recrystallized to give a second crop, 0.14 g (15%). ¹H NMR (600 MHz, C₆D₆): major signals appeared at δ 10.3 (Ph), 7.8 (SiMe₃), 5.3 (SiMe₃), −2.0 (Ph), −2.7 (SiMe₃), −3.8 (SiMe₃), −11.1 (Ph), −11.3 (Ph), −13.2 (Ph). UV–vis (cyclohexane): featureless with a slow rise toward the UV region. Anal. Calcd for C₄₈H₉₂Fe₄N₄S₄Si₈: C, 44.29; H, 7.12; N, 4.30; S, 9.85. Found: C, 43.89; H, 7.07; N, 3.82; S, 10.14. CV (1 mM in THF): E_{pc} = −1.99 V, E_{pa} = 0.23 V (irreversible).

Synthesis of [(Me₃Si)₂N]Fe₃(μ₃-O)(μ-SPh)₃ (3a). A toluene (25 mL) solution of HSPH (1.4 mL, 13.7 mmol) was added dropwise to a toluene (30 mL) solution of 1 (5.01 g, 13.3 mmol) at room temperature. After stirring for 1 h, O₂ (65 mL, 2.65 mmol) was bubbled into the mixture using a gas-tight syringe. The reaction mixture became a dark brown solution immediately. The mixture was stirred for 3 h at room temperature, and was evaporated to dryness under reduced pressure. The black residue was extracted with hexane (18 mL), and the extract was centrifuged to remove a small amount of insoluble material. Upon standing at room temperature, the solution deposited dark brown blocks of 3a (0.87 g, 20%). ¹H NMR (600 MHz, C₆D₆): δ 17.4 (6H, *o*- or *m*-H), 8.0 (54H, SiMe₃), −15.6 (3H, *p*-

H), −22.1 (6H, *o*- or *m*-H). UV–vis (hexane): λ_{max} = 241 nm (ε = 22000 M^{−1} cm^{−1}). Anal. Calcd for C₃₆H₆₉Fe₃N₃OS₃Si₆: C, 43.58; H, 7.01; N, 4.24; S, 9.70. Found: C, 43.34; H, 6.78; N, 3.92; S, 9.75. CV (20 mM in THF): E_{1/2} = −0.28, −1.20 V (quasi-reversible).

Synthesis of [(Me₃Si)₂N]Fe₃(μ₃-O)(μ-S(4'-BuC₆H₄))₃ (3b). Complex 3b was synthesized from 1 (5.09 g, 13.5 mmol), HS(4'-BuC₆H₄) (2.25 g, 13.5 mmol), and O₂ (66 mL, 2.69 mmol), in a similar manner to that used for 3a. Crystallization from hexane at −30 °C yielded dark brown blocks of 3b (2.72 g, 52%). ¹H NMR (600 MHz, C₆D₆): δ 17.5 (6H, *o*- or *m*-H), 7.9 (54H, SiMe₃), 1.1 (27H, ^tBu), −22.1 (6H, *o*- or *m*-H). UV–vis (hexane): λ_{max} = 241 nm (ε = 30000 M^{−1} cm^{−1}). Anal. Calcd for C₄₈H₉₃Fe₃N₃OS₃Si₆: C, 49.68; H, 8.08; N, 3.62; S, 8.29. Found: C, 49.40; H, 7.74; N, 3.63; S, 7.95. CV (20 mM in THF): E_{1/2} = −0.33, −1.25 V (quasi-reversible).

Synthesis of [(Me₃Si)₂N]Fe₂(μ-SDpp)(μ₃-O)₂ (4). A toluene (10 mL) solution of HSDpp (0.59 g, 2.25 mmol) was added dropwise to a toluene (10 mL) solution of 1 (0.85 g, 2.26 mmol) at room temperature. After stirring for 2 h, O₂ (17 mL, 0.69 mmol) was bubbled into the solution using a gas-tight syringe at room temperature. The resultant dark purple solution was stirred for 3 h at room temperature to afford a dark reddish brown solution. The solvent was removed under reduced pressure to give a black solid. The black residue was extracted with toluene (5 mL), and the extract was centrifuged to remove a small amount of insoluble material. Hexane (15 mL) was layered on the solution to yield black blocks of 4·C₆H₁₄ (0.18 g, 21%). Cooling the mother liquor at −40 °C resulted in the formation of colorless crystals of DppS–SDpp (0.12 g, 20%), which were identified by X-ray diffraction analysis. ¹H NMR (600 MHz, C₆D₆): major signals appeared at δ 25.5 (SiMe₃), 5.1 (SiMe₃), 4.4 (SiMe₃), 3.5 (Dpp), 2.8 (Dpp), 2.3 (Dpp), −1.8 (SiMe₃), −9.2 (Dpp), −16.4 (Dpp). UV–vis (hexane): λ_{max} = 419 nm (ε = 6000 M^{−1} cm^{−1}). Anal. Calcd for C₆₀H₉₈Fe₄N₄O₂S₂Si₈: C, 50.76; H, 6.96; N, 3.95; S, 4.52. Found: C, 51.10; H, 7.19; N, 3.58; S, 4.03. CV (2 mM in THF): E_{pc} = −2.48 V (irreversible).

Synthesis of DppS–SDpp. The synthetic procedure reported by Takaguchi et al.²⁵ was modified as follows. HSDpp (0.89 g, 3.39 mmol) was dissolved in 30 mL of CHCl₃. A CHCl₃ (30 mL) solution of Et₃N (0.7 mL, 5.02 mmol) was added to the CHCl₃ solution of HSDpp. A CHCl₃ solution (50 mL) of I₂ (0.86 g, 3.39 mmol) was

added to the reaction mixture to give a brown solution. The mixture was stirred for 3 h at room temperature, and was washed with aqueous saturated $\text{Na}_2\text{S}_2\text{O}_3$. The organic layer was dried over MgSO_4 and was evaporated until dryness. The product was isolated as colorless crystals (0.56 g, 63%) from a mixture of CH_2Cl_2 and EtOH at -40°C . ^1H NMR (600 MHz, CDCl_3): δ 7.33 (t, $J_{\text{H-H}} = 7.6$ Hz, 2H, *p*-CH of Dpp), 7.27 (m, 4H, *p*-CH of Ph), 7.20 (m, 8H, *o*- or *m*-CH of Ph), 7.09 (d, $J_{\text{H-H}} = 7.6$ Hz, 4H, *m*-CH of Dpp), 6.74 (m, 8H, *o*- or *m*-CH of Ph). $^{13}\text{C}\{^1\text{H}\}$ NMR (151 MHz, CDCl_3): δ 148.1, 141.7, 133.1, 130.1, 130.0, 128.4, 127.5, 126.7. UV-vis (hexane): $\lambda_{\text{max}} = 298$ nm ($\epsilon = 4500 \text{ M}^{-1} \text{ cm}^{-1}$), 337 nm ($\epsilon = 2100 \text{ M}^{-1} \text{ cm}^{-1}$). Anal. Calcd for $\text{C}_{36}\text{H}_{26}\text{S}_2$: C, 82.72; H, 5.01; S, 12.27. Found: C, 82.20; H, 5.41; S, 12.41. CV (4 mM in THF): $E_{\text{pc}} = -2.23$ V (irreversible). Melting point = $206\text{--}209^\circ\text{C}$.

Synthesis of $\{[(\text{Me}_3\text{Si})_2\text{N}](\text{TipS})(\text{THF})\text{Fe}_2(\mu\text{-O})\}$ (5). A THF (15 mL) solution of HSTip (3.21 g, 13.6 mmol) was added dropwise to a THF (15 mL) solution of **1** (5.11 g, 13.6 mmol) at room temperature. After stirring for 1 h, O_2 (100 mL, 4.08 mmol) was bubbled into the solution using a gas-tight syringe at -40°C . The reaction mixture became a dark red solution immediately. The mixture was allowed to warm to room temperature and was stirred for 6 h at room temperature. The solvent was removed under reduced pressure to give a dark red solid. The dark red residue was extracted with a mixture of HMDSO (38 mL) and THF (15 mL), and the extract was centrifuged to remove a small amount of insoluble material. Upon standing at -30°C , red needles of **5** (0.80 g, 11%) were formed. ^1H NMR (600 MHz, C_6D_6): major signals appeared at δ 35.4, 29.2, 21.2, 14.3, 5.3, 2.6 (SiMe_3), -3.8 . UV-vis (hexane): $\lambda_{\text{max}} = 280$ nm ($\epsilon = 9200 \text{ M}^{-1} \text{ cm}^{-1}$), 330 nm ($\epsilon = 6300 \text{ M}^{-1} \text{ cm}^{-1}$), 429 nm ($\epsilon = 6100 \text{ M}^{-1} \text{ cm}^{-1}$). Anal. Calcd for $\text{C}_{50}\text{H}_{98}\text{Fe}_2\text{N}_2\text{O}_3\text{Si}_4$: C, 56.47; H, 9.29; N, 2.63; S, 6.03. Found: C, 56.84; H, 9.53; N, 2.23; S, 6.53. CV (2 mM in THF): $E_{\text{pc}} = -1.65$ V (irreversible).

X-ray Crystal Structure Determination. Crystallographic data and refinement parameters for **2–5** and DppS–SDpp are summarized in Table 1. Single crystals were coated with oil (immersion Oil, type B: Code 1248, Cargille laboratories, Inc.) and mounted on loops. Diffraction data were collected at -100°C under a cold nitrogen stream on a Rigaku AFC8 equipped with a Rigaku Saturn 70 CCD/Micromax using graphite-monochromatized Mo $K\alpha$ radiation ($\lambda = 0.710690 \text{ \AA}$). Six preliminary data frames were measured at 0.5° increments of ω , to assess crystal quality and preliminary unit cell parameters. The intensity images were also measured at 0.5° intervals of ω . The frame data were integrated using the CrystalClear program package, and the data sets were corrected for absorption using a REQAB program. The calculations were performed with the CrystalStructure program package. All structures were solved by direct methods and refined by full-matrix least-squares. Anisotropic refinement was applied to all non-hydrogen atoms except for disordered atoms (refined isotropically), and all hydrogen atoms were put at calculated positions. Four ^tBu groups in **3b** are disordered over two positions in 1:1, 1:1, 2:3, or 1:1 ratios. Six Me_3Si groups in **3b** are disordered over two positions in 1:1, 7:3, 1:1, 1:1, 3:2, or 7:3 ratios. A SIMU restraint was applied to the C71–C76 atoms in **3b**.

■ ASSOCIATED CONTENT

■ Supporting Information

Crystallographic data in CIF format. This material is available free of charge via the Internet at <http://pubs.acs.org>.

■ AUTHOR INFORMATION

Corresponding Author

*E-mail: i45100a@nucc.cc.nagoya-u.ac.jp.

Notes

The authors declare no competing financial interest.

■ ACKNOWLEDGMENTS

This research was financially supported by the Grant-in-Aid for Specially Promoted Research (No. 23000007) from the

Ministry of Education, Culture, Sports, Science, and Technology, Japan. We thank Roger E. Cramer for his help in X-ray crystallographic analysis and for careful reading of the manuscript.

■ REFERENCES

- (1) Reviews: (a) Rao, P. V.; Holm, R. H. *Chem. Rev.* **2004**, *104*, 527–559. (b) Holm, R. H. *Comprehensive Coordination Chemistry II*; McCleverty, J. A., Meyer, T. L., Eds.; Elsevier Pergamon: Amsterdam, The Netherlands, 2004; Vol. 8, Chapter 8.3.
- (2) For example: (a) Han, S.; Czernuszewicz, R. S.; Spiro, T. G. *Inorg. Chem.* **1986**, *25*, 2276–2277. (b) Kanatzidis, M. G.; Hagen, W. R.; Dunham, W. R.; Lester, R. K.; Coucouvanis, D. *J. Am. Chem. Soc.* **1985**, *107*, 953–961. (c) Kanatzidis, M. G.; Dunham, W. R.; Hagen, W. R.; Coucouvanis, D. *J. Chem. Soc., Chem. Commun.* **1984**, 356–358. (d) Hagen, K. S.; Watson, A. D.; Holm, R. H. *J. Am. Chem. Soc.* **1983**, *105*, 3905–3913. (e) Hagen, K. S.; Holm, R. H. *J. Am. Chem. Soc.* **1982**, *104*, 5496–5497. (f) Hagen, K. S.; Reynolds, J. G.; Holm, R. H. *J. Am. Chem. Soc.* **1981**, *103*, 4054–4063. (g) Reynolds, J. G.; Holm, R. H. *Inorg. Chem.* **1980**, *19*, 3257–3260.
- (3) (a) MacDonnell, F. M.; Ruhlandt-Senge, K.; Ellison, J. J.; Holm, R. H.; Power, P. P. *Inorg. Chem.* **1995**, *34*, 1815–1822. (b) Ellison, J. J.; Ruhlandt-Senge, K.; Power, P. P. *Angew. Chem., Int. Ed. Engl.* **1994**, *33*, 1178–1180. (c) Ruhlandt-Senge, K.; Power, P. P. *Bull. Soc. Chim. Fr.* **1992**, *129*, 594–598. (d) Power, P. P.; Shoner, S. C. *Angew. Chem., Int. Ed. Engl.* **1991**, *30*, 330–332.
- (4) (a) Ohki, Y.; Imada, M.; Murata, A.; Sunada, Y.; Ohta, S.; Honda, M.; Sasamori, T.; Tokitoh, N.; Katada, M.; Tatsumi, K. *J. Am. Chem. Soc.* **2009**, *131*, 13168–13178. (b) Ohta, S.; Ohki, Y.; Ikagawa, Y.; Suizu, R.; Tatsumi, K. *J. Organomet. Chem.* **2007**, *692*, 4792–4799. (c) Ohki, Y.; Ikagawa, Y.; Tatsumi, K. *J. Am. Chem. Soc.* **2007**, *129*, 10457–10465. (d) Ohki, Y.; Sunada, Y.; Honda, M.; Katada, M.; Tatsumi, K. *J. Am. Chem. Soc.* **2003**, *125*, 4052–4053. (e) Komuro, T.; Kawaguchi, H.; Tatsumi, K. *Inorg. Chem.* **2002**, *41*, 5083–5090.
- (5) Hauptmann, R.; Kließ, R.; Schneider, J.; Henkel, G. Z. *Anorg. Allg. Chem.* **1998**, *624*, 1927–1936.
- (6) (a) Sydora, O. L.; Henry, T. P.; Wolczanski, P. T.; Lobkovsky, E. B.; Rumberger, E.; Hendrickson, D. N. *Inorg. Chem.* **2006**, *45*, 609–626. (b) Sydora, O. L.; Wolczanski, P. T.; Lobkovsky, E. B. *Angew. Chem., Int. Ed.* **2003**, *42*, 2685–2687.
- (7) Pryadun, R.; Holm, R. H. *Inorg. Chem.* **2008**, *47*, 3366–3370.
- (8) (a) Zdzila, M. J.; Verma, A. K.; Lee, S. C. *Inorg. Chem.* **2011**, *50*, 1551–1562. (b) Verma, A. K.; Lee, S. C. *J. Am. Chem. Soc.* **1999**, *121*, 10838–10839.
- (9) (a) Cooper, S. J.; Garner, C. D.; Hagen, W. R.; Lindley, P. F.; Bailey, S. *Biochemistry* **2000**, *39*, 15044–15054. (b) Arendsen, A. F.; Hadden, J.; Card, G.; McAlpine, A. S.; Bailey, S.; Zaitsev, V.; Duke, E. H. M.; Lindley, P. F.; Kröckel, M.; Trautwein, A. X.; Feiters, M. C.; Charnock, J. M.; Garner, C. D.; Marritt, S. J.; Thomson, A. J.; Kooter, I. M.; Johnson, M. K.; Van Den Berg, W. A. M.; Van Dongen, W. M. A. M.; Hagen, W. R. *J. Biol. Inorg. Chem.* **1998**, *3*, 81–95.
- (10) Hagen, W. R.; Pierik, A. J.; Veeger, C. *J. Chem. Soc., Faraday Trans. 1* **1989**, *85*, 4083–4090.
- (11) Einsle, O.; Tezcan, F. A.; Andrade, S. L. A.; Schmid, B.; Yoshida, M.; Howard, J. B.; Rees, D. C. *Science* **2002**, *297*, 1696–1700.
- (12) Review: Cannon, R. D.; White, R. P. *Prog. Inorg. Chem.* **1988**, *36*, 195–297.
- (13) For recent references, see: (a) Novitchi, G.; Riblet, F.; Scopelliti, R.; Helm, L.; Gulea, A.; Merbach, A. E. *Inorg. Chem.* **2008**, *47*, 10587–10599. (b) Marchetti, F.; Marchetti, F.; Melai, B.; Pampaloni, G.; Zacchini, S. *Inorg. Chem.* **2007**, *46*, 3378–3384. (c) Dai, J.-X.; Wu, F.-H.; Rothenberger, A.; Zhang, Q.-F. *Z. Naturforsch., B: Chem. Sci.* **2007**, *62*, 1117–1122. (d) Saalfrank, R. W.; Scheurer, A.; Reimann, U.; Hampel, F.; Trieflinger, C.; Büschel, M.; Daub, J.; Trautwein, A. X.; Schünemann, V.; Coropceanu, V. *Chem.—Eur. J.* **2005**, *11*, 5843–5848. (e) Burkill, H. A.; Robertson, N.; Vilar, R.; White, A. J. P.; Williams, D. J. *Inorg. Chem.* **2005**, *44*, 3337–3346.

(14) For example: (a) Reynolds, R. A. III; Dunham, W. R.; Coucouvanis, D. *Inorg. Chem.* **1998**, 37, 1232–1241. (b) Poganiuch, P.; Liu, S.; Papaefthymiou, G. C.; Lippard, S. J. *J. Am. Chem. Soc.* **1991**, 113, 4645–4651.

(15) Nguyen, T.; Panda, A.; Olmstead, M. M.; Richards, A. F.; Stender, M.; Brynda, M.; Power, P. P. *J. Am. Chem. Soc.* **2005**, 127, 8545–8552.

(16) For recent references, see: (a) Rabe, V.; Frey, W.; Baro, A.; Laschat, S.; Bauer, M.; Bertagnolli, H.; Rajagopalan, S.; Asthalter, T.; Roduner, E.; Dilger, H.; Glaser, T.; Schnieders, D. *Eur. J. Inorg. Chem.* **2009**, 4660–4674. (b) Mereacre, V.; Prodius, D.; Ako, A. M.; Shova, S.; Turta, C.; Wurst, K.; Jaitner, P.; Powell, A. K. *Polyhedron* **2009**, 28, 3551–3555. (c) Gkioni, C.; Boudalis, A. K.; Sanakis, Y.; Psycharis, V.; Raptopoulou, C. P. *Polyhedron* **2009**, 28, 3221–3226. (d) Abunawwas, A.-A. H.; Muryn, C. A.; Malik, M. A. *Inorg. Chem. Commun.* **2009**, 12, 125–127. (e) Hearn, N. G. R.; Fatila, E. M.; Clérac, R.; Jennings, M.; Preuss, K. E. *Inorg. Chem.* **2008**, 47, 10330–10341.

(17) Reviews: (a) Tshuva, E. Y.; Lippard, S. J. *Chem. Rev.* **2004**, 104, 987–1012. (b) Kurtz, D. M. Jr. *Chem. Rev.* **1990**, 90, 585–606.

(18) Recent examples: (a) Koike, T.; Yokota, S.; Fujiwara, H.; Sugimoto, T.; Noguchi, S.; De Caro, D.; Valade, L. *Inorg. Chem.* **2008**, 47, 7074–7076. (b) Thallaj, N. K.; Rotthaus, O.; Benhamou, L.; Humbert, N.; Elhabiri, M.; Lachkar, M.; Welter, R.; Albrecht-Gary, A.-M.; Mandon, D. *Chem.—Eur. J.* **2008**, 14, 6742–6753. (c) Çelenligil-Çetin, R.; Paraskevopoulou, P.; Dinda, R.; Lalioti, N.; Sanakis, Y.; Rawashdeh, A. M.; Staples, R. J.; Sinn, E.; Stavropoulos, P. *Eur. J. Inorg. Chem.* **2008**, 673–677. (d) Kermagoret, A.; Tomicki, F.; Braunstein, P. *Dalton Trans.* **2008**, 2945–2955. (e) Pilz, M. F.; Limberg, C.; Demeshko, S.; Meyer, F.; Ziemer, B. *Dalton Trans.* **2008**, 1917–1923.

(19) For example: (a) Girma, K. B.; Lorenz, V.; Blaurock, S.; Edelmann, F. T. *Inorg. Chim. Acta* **2008**, 361, 346–348. (b) Neuba, A.; Akin, E.; Herres-Pawlis, S.; Flörke, U.; Henkel, G. *Acta Crystallogr.* **2008**, C64, m194–m197.

(20) Jinhua, C.; Jiaxi, L. *Jiegou, Huaxue* **1988**, 7, 57–60.

(21) Pangborn, A. B.; Giardello, M. A.; Grubbs, R. H.; Rosen, R. K.; Timmers, F. J. *Organometallics* **1996**, 15, 1518–1520.

(22) Ohki, Y.; Ohta, S.; Tatsumi, K. *Inorg. Synth.* **2010**, 35, 137–143.

(23) Bishop, P. T.; Dilworth, J. R.; Nicholson, T.; Zubieta, J. J. *Chem. Soc., Dalton Trans.* **1991**, 385–392.

(24) (a) Blower, P. J.; Dilworth, J. R.; Hutchinson, J. P.; Zubieta, J. A. *J. Chem. Soc., Dalton Trans.* **1985**, 1533–1541. (b) Miller, A. R.; Curtin, D. Y. *J. Am. Chem. Soc.* **1976**, 98, 1860–1865.

(25) Tsuboi, T.; Takaguchi, Y.; Tsuboi, S. *Bull. Chem. Soc. Jpn.* **2008**, 81, 361–368.